

Land Use Change Monitoring in Haidian District Based on Remote Sensing Data

Lijun Tian¹, Chenxuan Zhao²

¹Department of Mining Engineering, North China University of Science and Technology, Tangshan, 063210, China

²Department of Civil Engineering, Shijiazhuang Tiedao University, Shijiazhuang, 050043, China

Abstract: For urban planning and sustainable development, monitoring land use change is essential. Based on the Sentinel-2 series data from the ESA, this study inverted the vegetation coverage of the study region using the binary pixel model. It classified the ground objects in Haidian District from 2018 to 2021 with the maximum likelihood method. This work has dynamically tracked the fluctuating ground features and vegetation in the Haidian District. The monitoring results show that the overall area of water has not changed much in the past four years. Since 2019, the scope of building land has shown a slowly decreasing trend. The extent of woodland and the bare ground has reduced yearly, and the rate of decrease was similar. The urban center of gravity mainly shifted from southeast to northwest during 2018-2019. From 2019 to 2021, the center of gravity moved slightly to the east. Vegetation coverage gradually increased from the city's edge to the city center. This study can provide a reference for the construction planning and ecological protection of Beijing's central cities.

Keywords: Land Use Change, Supervised Classifications, Maximum Likelihood Method

1. Introduction

Remote sensing technology is widely used in urban monitoring because it can provide dynamic, rich, and large-scale data information [1]. Remote sensing dynamic monitoring is based on the detection of qualitative and quantitative information on the spatial distribution of features and their changes, which in turn leads to further analysis and exploration of the change information.

Against the backdrop of increasing pressure on the capital city due to urban expansion, Beijing has been adhering to the strategy of "reduced development" in recent years. The effectiveness of this initiative can be easily seen through remote sensing imagery. And the dynamic change in land use has become a critical problem to be solved in studying global environmental change [2]. Due to the significant spatial heterogeneity of land use, it is time-consuming and laborious to monitor it by traditional methods. The accuracy cannot be guaranteed. Therefore, the efficient use of remote sensing images for land use change monitoring has become a hot issue for many scholars.

At this stage, remote sensing monitoring technology continues to develop. Bin Hou proposed a saliency-guided semi-supervised building change detection method for high-resolution remote sensing images [3]. Jiadi Yin[4] conducted researches on the urban green space pattern change under land use change in Hangzhou. Based on Random Forest (RF) algorithm, Xuan Guo integrated Vietnam's land use/cover data for nearly 21 years [5]. M Castelluccio[6] performed land use classification of remote sensing images based on a convolutional neural network.

This paper uses the ESA's Sentinel-2 series data to classify the ground objects in Haidian District from 2018 to 2021 by using the maximum likelihood method, and compare the classification results to analyze the law of urban land use change. On this basis, using the vegetation coverage inversion model, the dynamic time-series monitoring of vegetation coverage in Haidian District from 2018 to 2021 is carried out.

2. Research data and methods

2.1 Overview of the study area

The Haidian District is located in the west and northwest of Beijing. The terrain is mainly mountains

and plains and the four seasons are distinct. Figure 1 depicts the area of this paper's research.

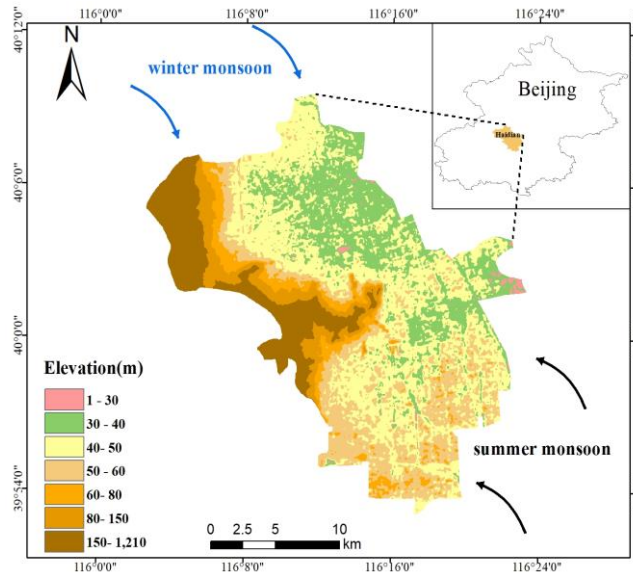


Figure 1: Overview of the study area

2.2 Data Sources

The data in the study area is the L1C level of the Sentinel-2 series data launched by ESA. On the ESA's official website, this article downloads four years' higher-quality photos from 2018 to 2021. The data used is as Table 1 shows.

Table 1: Time distribution of data

Spring	Summer	Autumn	Winter
Apr. 8,2018	May. 28,2018	Oct. 30,2018	Jan. 23,2019
Apr. 3,2019	May. 28,2019	Sept. 25,2019	Nov. 19,2019
Mar. 23,2020	Jun. 6,2020	Sept. 19,2020	Dec. 3,2020
Apr. 7,2021	Jun. 21,2021	Sept. 29,2021	Dec. 3,2021

2.3 Research method

2.3.1 Image processing flow

In this paper, 16 scenes are resampled to 10m, common bands are selected and cut according to the vector boundary. In ENVI, the maximum likelihood method is used to classify the study area, and land use change monitoring is carried out according to the classification results. Furthermore, using NDVI from the summer of 2018-2021 to calculate FVC. The flow chart is in Figure 2.

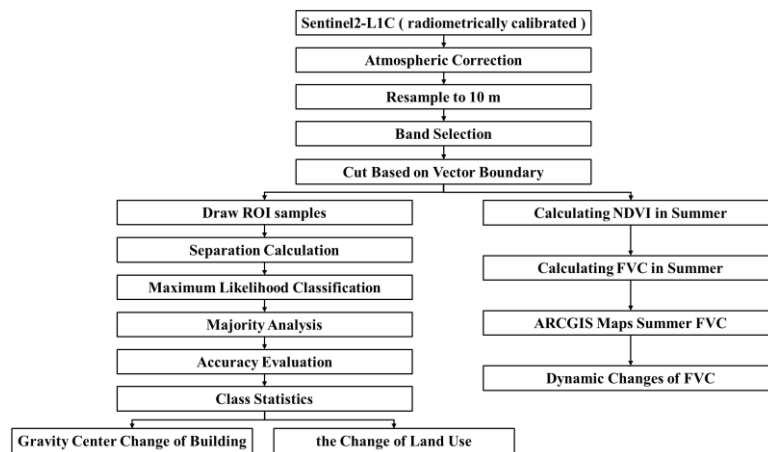


Figure 2: Image processing flow

2.3.2 Supervised Classification Model Based on Maximum Likelihood

Supervised classification is artificially referenced by expert experience or higher-resolution images. Then the computer learns the sample set based on the spectral characteristics of the ground object. K Perumal[7] studied the supervised classification performance of multispectral images. The specific classification formula is (1).

$$D = \ln \beta_{\omega} - [0.5 \ln(|Cov_{\omega}|)] - [0.5(X - M_{\omega})^T (Cov_{\omega})^{-1} (X - M_{\omega})] \quad (1)$$

In the formula, D is the weighted distance. ω is classification. M_{ω} is the average value of ω . Cov_{ω} and $|Cov_{\omega}|$ are respectively the covariance matrix and determinant of ω . X is the pixel measurement vector.

2.3.3 Land use dynamics

Sun Jing Wen[8] analyzed land use dynamics in Genhe City based on GIS and RS. The single land use dynamic attitude tends to be more a reflection of time-domain change, indicating the rate of change in area for a particular land use type in the study area. Its calculation formula is (2).

$$\delta = \frac{S_1 - S_2}{S_1} \times \frac{1}{\tau} \times 100\% \quad (2)$$

Where δ is the dynamic degree of a single land use type in the time domain of τ ; S_1 and S_2 are the area of a certain land type at the beginning of the study and at the end of the study, respectively.

2.3.4 Vegetation Coverage Calculation

Normalized vegetation index is an important index for studying vegetation growth, which can provide valuable information about vegetation distribution, productivity, and dynamic spatio-temporal changes [9]. The calculation formula is (3).

$$NDVI = \frac{f_{NIR} - f_R}{f_{NIR} + f_R} \quad (3)$$

In the formula, f_{NIR} is the reflection value of the near-infrared band, and f_R is the reflection value of the red band.

Z Li [10] found that when the vegetation coverage exceeded 60%, the development of bank gully was significantly controlled. In 2004, Miaomiao Li proposed an improved pixel dichotomy model, and the calculation formula is (4).

$$FVC = \frac{NDVI - NDVI_{\min}}{NDVI_{\max} - NDVI_{\min}} \quad (5)$$

In the formula: FVC is the vegetation coverage; NDVI is the pixel NDVI value. In this paper, $NDVI_{\max}$ with a frequency of 90% was used as the NDVI value of pure vegetation coverage. The frequency of 5% $NDVI_{\min}$ was used as the NDVI value of pure bare soil.

3. Result

3.1 Analysis of classification results and evaluation

By using the maximum likelihood method to classify the study area, the classification results from 2018 to 2021 are shown in Figure 3. By comparing the higher-resolution real-world map of Haidian District, this paper calculated the overall classification accuracy and Kappa coefficient of the 16 phase images. It can be found from the results that the overall classification accuracy is above 90%.

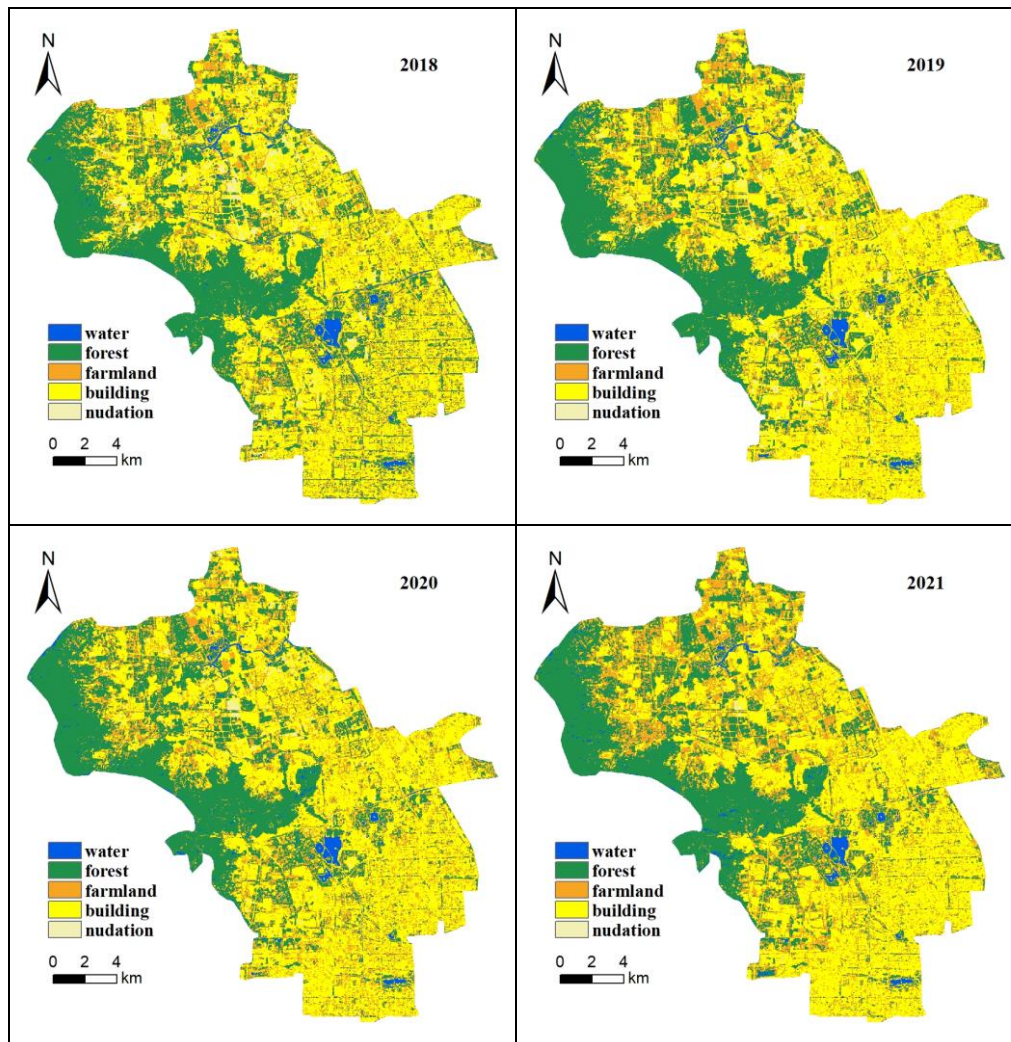


Figure 3: Land classification results for 2018-2021

Figure 4 lists the annual average area trends of the five surface object types in the study area from 2018 to 2021.

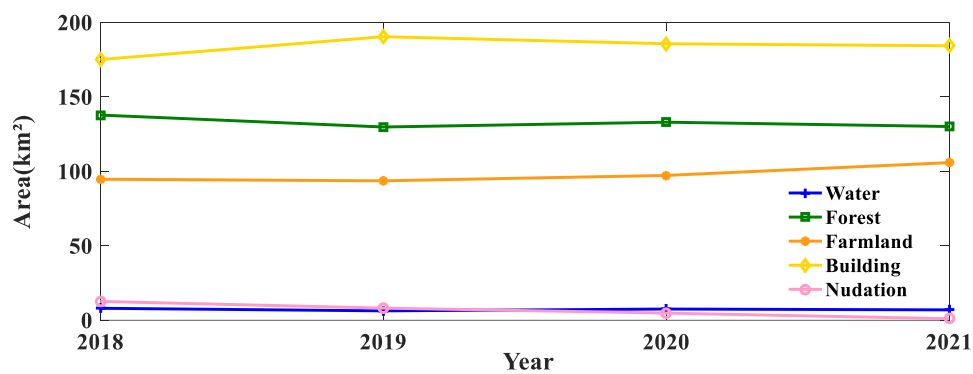


Figure 4: Trend of annual average area of 5 land types

It can be seen from the figure that the construction land is mainly concentrated in the southeast of the city, followed by the north. Woodlands are mainly concentrated in the west. The bare land is distributed scattered in the north of the center. There are also some cultivated lands in the northern edge and central area. The water of Haidian District is distributed in a certain amount in the north and south.

3.2 Changes in average surface feature types from 2018 to 2021

As can be seen from Figure 5, the area of arable land in Haidian District has shown an overall increasing trend over the four years, except for a slight fluctuation in 2019. The growth rate of cultivated land has become faster with time. Thanks to the "dual control" strategy of population and construction scale that Beijing has focused on in recent years, since 2019, the area of construction land has shown a slow decreasing trend. The overall water area has not changed much in the past four years. The area of forest land and bare land decreased yearly, and the rate of decrease was similar.

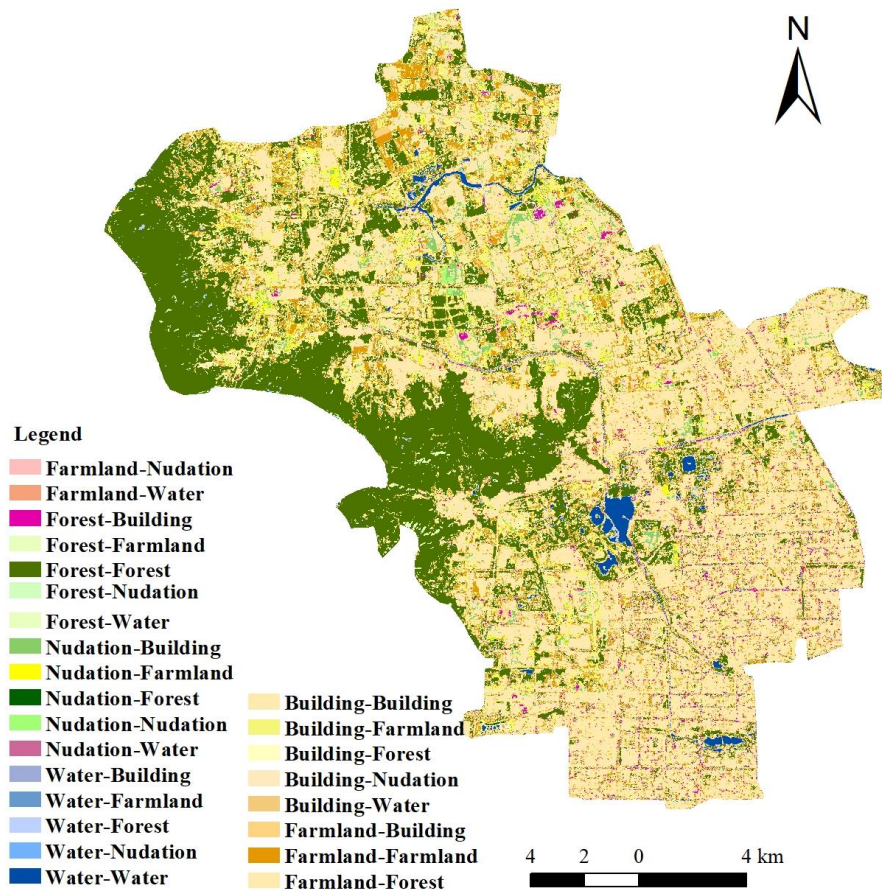


Figure 5: Comparison of land use results in 2018 and 2021

The land use type transition matrix in 2018 and 2021 is shown in Table 2. It is found that compared with 2018, the increased building area is mainly from the conversion of farmland. About 67% of the cultivated land was transformed into construction land. Table 3 shows that the mutual transformation between cultivated land and buildings is relatively apparent. Compared with 2021, the change of land use type in 2018 is mainly manifested in: the net increase of construction land area is 7.94 km² of which the reduction of construction land is mainly transferred to cultivated land (88.59%), and a very small amount of water is reclaimed as construction land. During the four years, the area of cultivated land transferred is the largest. Most of the increased cultivated land is converted from construction land (54.78%) and forest land (36.30%). From 2018 to 2021, the size of the total change in area for each land use category in the study area is in the order of arable land > building land > woodland > bare land > watersheds.

Table 2: Transfer matrix of classified land use

Unit: Km²

	Building	Farmland	Forest	Nudation	Water
Building	138.92	33.11	3.66	0.55	0.05
Farmland	30.41	45.33	17.71	0.09	0.24
Forest	7.16	21.94	106.50	0.03	2.07
Nudation	7.30	4.36	0.33	0.33	0.01
Water	0.44	1.02	1.78	6.40×10^{-5}	4.55

Table 3: Land use dynamic degrees

	Roll-out /km ²	Roll-in /km ²	Total Change /km ²	Area Variation /km ²	δ (%)
Building	37.37	45.31	82.68	7.94	1.32
Farmland	48.44	60.44	108.88	12.00	2.94
Forest	31.21	23.48	54.69	-7.73	-1.39
Nudation	12.01	0.68	12.68	-11.33	-23.00
Water	3.24	2.37	5.61	-0.87	-3.33

3.3 Average Building Center of Gravity Migration and Error Ellipse for 2018-2021

As shown in Figure 6, it can be found that the city's center of gravity has changed significantly from 2018 to 2019, and the distance of the gravity shift is the longest, mainly from the southeast to the northwest. From 2019 to 2021, the center of gravity shifted slightly to the east.

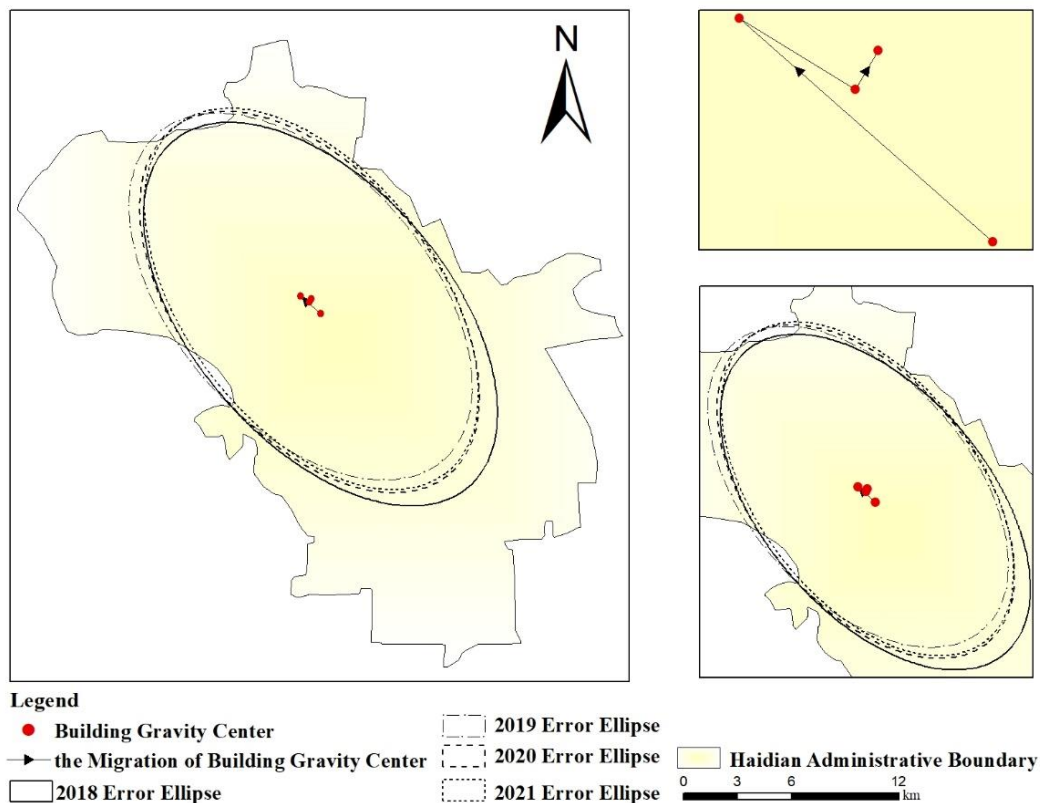


Figure 6: The center of gravity change of buildings

3.4 Summer FVC changes in 2018-2021

To better observe the dynamic changes of vegetation coverage in the study area, selecting the summer with lush vegetation in four years as the time series. In Figure 7, (a)-(d) respectively represent the temporal-spatial distribution of FVC during 2018-2021. The results show that the vegetation coverage gradually increases from the city edge to the city center. The areas with higher vegetation coverage are concentrated on the western edge of Haidian District, while the eastern part is characterized by low vegetation coverage due to dense construction.

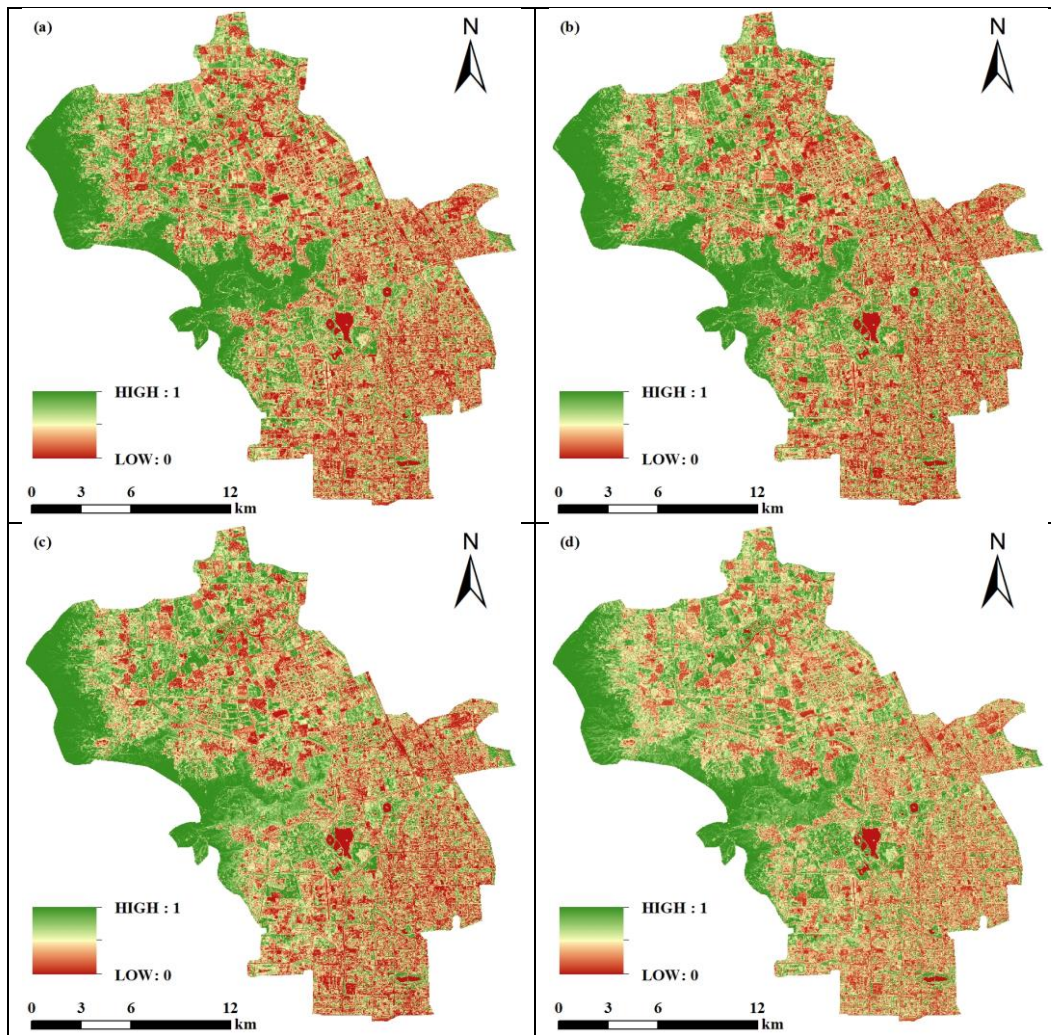


Figure 7: Temporal spatial distribution of FVC

4. Conclusion

This paper takes Haidian District of Beijing as an example, analyzing the change in vegetation coverage and the trend of coverage offset from 2018 to 2021, and using the supervised classification model of the maximum likelihood method to summarize the spatial distribution characteristics in four years. The result shows:

(1) Vegetation coverage gradually increases from the city's edge to the city center. The building's gravity shift distance in Haidian District decreased with time lag from 2018 to 2021.

(2) The size of the total change in area for each land use category in the study area is in the order of arable land > building land > woodland > bare land > watersheds.

The image data source in this paper is relatively single, so the application scope of experimental results has certain limitations. However, it can still provide reference for the sustainable development of Haidian District.

References

- [1] Liu Sai. *Spatial distribution characteristics of urban landscape pattern based on multi-source remote sensing technology [J]. International Journal of Environmental Technology and Management*, 2021, 24 (1a2): 33-48.
- [2] Ji Yuan, Liu Mingliang, et al. *Study on spatial pattern of land-use change in China during 1995–2000[J]. Science in China*, 2003.

- [3] Hou B.; Wang Y.; Liu Q. A Saliency Guided Semi-Supervised Building Change Detection Method for High Resolution Remote Sensing Images. *Sensors* 2016, 16, 1377.
- [4] Yin J.; Fu P.; Cheshmehzangi A.; Li Z.; Dong J. Investigating the Changes in Urban Green-Space Patterns with Urban Land-Use Changes: A Case Study in Hangzhou, China. *Remote Sens.* 2022, 14, 5410.
- [5] Guo X.; Ye J.; Hu Y. Analysis of Land Use Change and Driving Mechanisms in Vietnam during the Period 2000–2020. *Remote Sens.* 2022, 14, 1600.
- [6] Castelluccio M, Poggi G, Sansone C, et al. Land Use Classification in Remote Sensing Images by Convolutional Neural Networks[J]. *Acta Ecologica Sinica*, 2015, 28(2):627-635.
- [7] Perumal K, Bhaskaran R. Supervised Classification Performance of Multispectral Images: 10.48550/arXiv. 1002.4046[P]. 2010.
- [8] Sun J W, Wang H Q, Zhang Y F. Analysis of Land Use Dynamic in Genhe City Based on GIS and RS. *AMM* 2012; 256–259:2298–302.
- [9] Pettorelli N. *The Normalized Difference Vegetation Index [M]*. 2013.
- [10] Li Z, Zhang Y, Zhu Q, et al. Assessment of bank gully development and vegetation coverage on the Chinese Loess Plateau [J]. *Geomorphology*, 2015, 228:462-469.